

## First- and Second-Order Closure Models for Wind in a Plant Canopy

J. D. JEAN-PAUL PINARD AND JOHN D. WILSON

*Department of Earth and Atmospheric Sciences, University of Alberta, Edmonton, Alberta, Canada*

(Manuscript received 19 October 2000, in final form 26 February 2001)

### ABSTRACT

Katul and Chang recently compared the performance of two second-order closure models with observations of wind and turbulence in the Duke Forest canopy, noting that such models “alleviate some of the theoretical objections to first-order closure.” This paper demonstrates that, notwithstanding those (valid) theoretical objections, Duke Forest wind simulations of comparable quality can be obtained using a first-order closure, namely, eddy viscosity  $K \propto \lambda \sqrt{k}$ , where  $k$  is the turbulent kinetic energy and  $\lambda$  is a turbulence length scale. It is concluded that, most often, uncertainty in the drag coefficient will limit the accuracy of modeled wind statistics, regardless of the turbulence closure chosen.

### 1. Introduction

As a precursor to rational scientific treatment of many forest processes, such as aerial spray dispersion or the spread of pollen or plant pathogens, profiles of mean horizontal wind velocity  $\bar{u}$  and turbulence statistics (e.g., component wind velocity variances  $\sigma_u^2$ ,  $\sigma_v^2$ , and  $\sigma_w^2$ ) need to be known. Furthermore these statistical properties of the wind modulate the relationship between the mean properties of the airstream (e.g., humidity and carbon dioxide concentration) and the rates of emission/absorption by the vegetation (leaf transpiration and photosynthesis). Thus atmosphere–forest interactions are of great importance in such fields as agronomy and forestry.

Dynamical models for wind in a “horizontally uniform” plant canopy, in which by definition flow statistics may vary with the height  $z$  but *not* along the horizontal coordinates, are based on a mean streamwise momentum equation,<sup>1</sup>

$$\frac{\partial \overline{u'w'}}{\partial z} = -C_d a \bar{u}^2 - \frac{\partial \bar{p}}{\partial x}, \quad (1)$$

where  $\overline{u'w'}$  is the mean vertical flux of streamwise momentum (Reynolds stress),  $C_d a \bar{u}^2$  parameterizes drag on plant parts [ $C_d = C_d(z)$  is the drag coefficient,  $a = a(z)$

is the leaf area density], and  $\partial \bar{p} / \partial x$  is (any) streamwise gradient in kinematic pressure. Wind models are distinguished as being of first- or second-order closure, according to their means of providing the Reynolds stress in Eq. (1).

Seeking “a practical framework for computing needed velocity statistics for modeling scalar transport,” Katul and Chang (1999, hereinafter KC99) compared two second-order closure models (Wilson and Shaw 1977, hereinafter WS77; and Wilson 1988, hereinafter W88) with measured winds in the Duke Forest of North Carolina. They concluded that WS77 produced a slightly better mean velocity profile  $\bar{u}$  but a worse standard deviation profile  $\sigma_u$  than did W88 and that the modeled third moments were inconsistent with measurements. Our point of departure with respect to KC99 is that, whereas these authors sought to establish which was the better second-order model of the two they compared, they did not enquire whether a first-order closure might have been comparably suitable. In raising this question, we do not dispute the logical superiority of second-order closures or overlook their promise to partition the turbulent kinetic energy  $k = 1/2(\sigma_u^2 + \sigma_v^2 + \sigma_w^2)$  into its components ( $\sigma_w^2$ , etc.); we merely wish to highlight ambiguities or uncertainties common to both approaches (e.g., optimal closure constants, means of providing the drag coefficient) and query whether these imply that the vaunted superiority of second-order closure is inconsequential. Thus our goal is to establish whether there is any striking gain in accuracy of modeling the first and second velocity moments when the more complex approach (second-order closure) is taken.

In what follows, we briefly review an existing first-order closure model for canopy flows (that of Wilson et al. 1998, hereinafter WFR98) and our numerical

<sup>1</sup> For a derivation see Wilson and Shaw (1977) or Raupach and Shaw (1982). In simplifying to obtain Eq. (1) we assumed the dispersive momentum flux to be negligible.

Corresponding author address: J. D. Jean-Paul Pinard, Department of Earth and Atmospheric Sciences, 1-26 Earth Sciences Building, University of Alberta, Edmonton, AB T6G 2E3, Canada.  
E-mail: jpinard@ualberta.ca

method for solving it. In section 3, we discuss the determination of the drag coefficient from measurements. In section 4, we compare our own simulations of the Duke Forest winds with the observations and simulations of KC99.

**2. A first-order closure model for wind in a uniform canopy**

A balance between the divergence of the mean vertical flux of streamwise momentum and drag on plant parts controls the airflow within a uniform canopy [Eq. (1)]. In a first-order (or “flux-gradient”) closure, turbulence is approximated as being equivalent to an increased viscosity of the fluid; that is, the shear stress is modeled as  $\overline{u'w'} = -K(\partial\overline{u}/\partial z + \partial\overline{w}/\partial x)$ , where the eddy viscosity  $K$  is determined by the flow itself. Our present assumption of a *uniform* canopy eliminates the term in mean vertical velocity.

Higher-order closures, such as those exploited by KC99, use the Navier–Stokes equations to obtain exact governing equations for  $\overline{u'w'}$  and other turbulence statistics—equations that are subsequently simplified so as to attain closure (as many equations as unknowns). Many mechanisms are thereby resolved exactly, for example, the shear production  $\overline{u'w'}(\partial\overline{u}/\partial z)$  and advection  $\overline{u}(\partial\overline{u'^2}/\partial x)$  of  $u$  variance; other mechanisms have to be approximated (for example, the triple moments  $\overline{u'_i u'_j u'_k}$  are often assumed to be fluxes driven by spatial gradients in  $u'_i u'_j$ ). Substitution of a higher-order closure for a first-order closure is a step in the direction of greater rigor. However, both types of models require empirical inputs that are somewhat uncertain (e.g., the drag coefficient), and it is our contention and the point of this paper that for many purposes the first-order closure model will be sufficient.

*a. Equations determining the eddy viscosity*

Our calculations will use the first-order closure of WFR98, who parameterized the eddy viscosity as  $K = \lambda(z)\sqrt{c_e k(z)}$ , where  $\lambda(z)$  is an algebraic length scale (defined below);  $c_e$  is a (fairly well known) quasi constant, giving the equilibrium shear-stress: turbulent kinetic energy (TKE) ratio ( $u_{z=0}^2/k_0$ ) immediately above the canopy; and  $k$  is the TKE, calculated from a simplified transport equation

$$\frac{\partial k}{\partial t} = 0 = -\overline{u'w'}\frac{\partial\overline{u}}{\partial z} + \frac{\partial}{\partial z}\left(\mu K\frac{\partial k}{\partial z}\right) - \varepsilon. \quad (2)$$

Here we neglect buoyant production, because our calculations pertain only to the case of neutral stratification. The effective diffusion coefficient for TKE,  $\mu K$ , is proportional to the eddy viscosity, and, as in WFR98, we set  $\mu = 0.2$ . The viscous dissipation is written as  $\varepsilon = \max(\varepsilon_{cc}, \varepsilon_{fd})$ , where  $\varepsilon_{cc} = (c_e k)^{3/2}/\lambda$  and  $\varepsilon_{fd} = \alpha C_d a \overline{u} k$ . The term  $\varepsilon_{cc}$  balances shear production of TKE in the

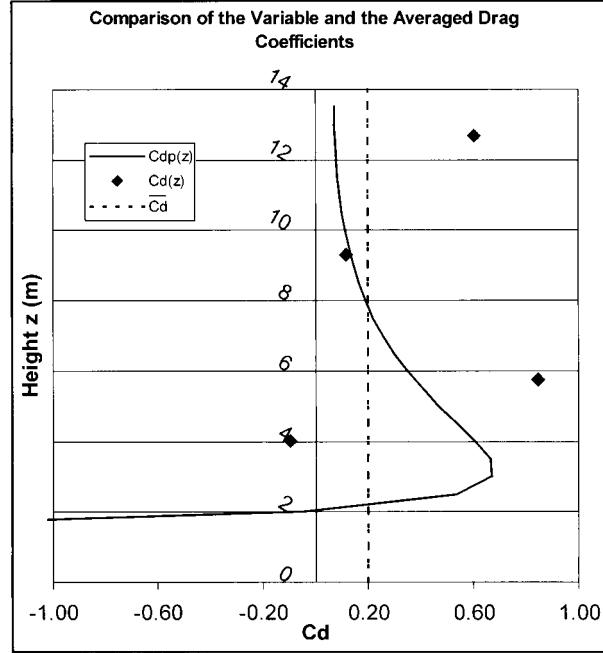


FIG. 1. The plot for (finite-difference based)  $C_d(z)$  is highly variable and shows how sensitive it can be to noise in the shear stress gradient. The calculated (polynomial based) drag coefficient  $C_{dp}(z)$  is negative at the ground and positive above  $z = 2$  m. The value for the height-averaged drag coefficient  $\overline{C_d}$ , which is the same for both our calculation and that of KC99, is shown for comparison.

local equilibrium layer far above the canopy (and is the standard parameterization for viscous dissipation). The form drag  $\varepsilon_{fd}$  represents conversion of resolved TKE to small, rapidly dissipated “wake scales,” and the closure constant  $\alpha$  was reasoned by WFR98 to be approximately equal to 1.

Crucial to the WFR98 closure is the specification of the length scale  $\lambda$ , which is characterized as the maximum of *inner* and *outer* length scales

$$\frac{1}{\lambda_i} = \frac{1}{k_v z} + \frac{1}{\lambda_c}, \quad \text{and} \quad (3a)$$

$$\frac{1}{\lambda_o} = \frac{1}{k_v(z-d)} + \frac{1}{L_\infty}. \quad (3b)$$

Here  $k_v = 0.4$  is the von Kármán constant and  $d$  is the displacement height (usually set as  $2/3$  of the canopy height  $h_c$ ). The outer scale  $\lambda_o$  recognizes the flow displacement by the canopy and, for the case of a wind-tunnel experiment, a finite limiting value  $L_\infty$ . The inner scale  $\lambda_i$  recognizes the limitation on eddy size due to proximity to ground and the presence of the canopy, which is felt through an upper limit  $\lambda_c$  to the inner length scale:

$$\lambda_c = c\sqrt{k(h_c)}\left(\frac{\partial\overline{u}}{\partial z}\right)_{h_c}^{-1}. \quad (4)$$

Equation (4) is based on the suggestion of Raupach et al. (1996) that the strength of the wind shear at the canopy height is critical to eddy transport within a canopy; WFR98 determined that the closure constant  $c$  is approximately equal to 1.0. Numerous other formulations of the eddy viscosity within and above a plant canopy have been suggested. The current one has been tested over a wider variety of *uniform* canopy flows than most and has been shown to perform very well for *disturbed* winds in forest clearings (Wilson and Flesch 1999).

### b. Partitioning TKE into its components

An advantage in principle of a second-order model is its ability to partition the TKE into its components ( $\sigma_u^2$ ,  $\sigma_v^2$ ,  $\sigma_w^2$ ) and thus to make specific predictions of flow statistics vital to canopy transport—especially  $\sigma_w(z)$ , which is a necessary input to Lagrangian stochastic dispersion models such as have recently been used to infer canopy source/sink strengths (e.g., for carbon dioxide) from measured concentration profiles. The  $K \propto \lambda \sqrt{k}$  closure does not offer this information, and the best one can easily do is to assume constant partitioning ratios  $\sigma_u^2/k = \gamma_u^2$ ,  $\sigma_v^2/k = \gamma_v^2$ , and  $\sigma_w^2/k = \gamma_w^2$ . The partitioning constants satisfy  $\gamma_u^2 + \gamma_v^2 + \gamma_w^2 = 2$  and allow us to write  $\sigma_u/u_* = \gamma_u/\sqrt{c_e}$ , and so on, where  $u_*$  is friction velocity. Note that the analytical second-order closure of Massman and Weil (1999) likewise assumed “that  $\sigma_u^2$ ,  $\sigma_v^2$ ,  $\sigma_w^2$  are each proportional to  $(k)$  and that the proportionality constants are the same as those at the canopy top.”

### c. Numerical method used to implement the $K$ -theory model

Discretization equations are formulated following the approach of Patankar (1980). The governing equations are integrated across a control layer spanning height range  $s \leq z \leq n$  to yield a “neighbor equation,” linking velocity at the  $J$ th grid point to its values above ( $J + 1$ ) and below ( $J - 1$ ). Our momentum equation, closed using  $K$  theory, upon such integration gives

$$\left[ -K \frac{\partial \bar{u}}{\partial z} \right]_s^n = -\Delta z C_J \bar{u}_J^2, \quad (5)$$

where  $C_J$  is the product of the drag coefficient and area density (see section 3). The momentum fluxes across the north ( $n$ ) and south ( $s$ ) faces are evaluated as

$$\begin{aligned} \left( K \frac{\partial \bar{u}}{\partial z} \right)_n &= K_n \frac{\bar{u}_{J+1} - \bar{u}_J}{\Delta z}, \\ \left( K \frac{\partial \bar{u}}{\partial z} \right)_s &= K_s \frac{\bar{u}_J - \bar{u}_{J-1}}{\Delta z}, \end{aligned} \quad (6)$$

and the resulting neighbor equation for velocity is

TABLE 1. Parameters of the Duke canopy experiments.

Property	Symbol	Value
Canopy height	$h_c$	14.0 m
Model height	Lid	$10h_c$
Bulk drag parameter calculated in section 3c	$C_{db} = \overline{C_d} a h_c$	0.34
Height-averaged drag coefficient from section 3b and as KC99	$\overline{C_d}$	0.2
Displacement height	$d/h_c$	0.67
Equilibrium variances as given by KC99	$\sigma_{u,v,w}/u_{*0}$	2.08, 1.86, 1.22
Closure coefficients	$c, \alpha, \mu$	1.0, 1.0, 0.2
Limit to length scale	$L_\infty$	1.5
Grid points/iterations		100/100

$$-A_n^u \bar{u}_{J+1}^m + A_c^u \bar{u}_J^m - A_s^u \bar{u}_{J-1}^m = \Delta z \left( -\frac{\partial \bar{p}}{\partial x} \right)_J, \quad (7)$$

where  $A_n^u = K_n/\Delta z$ ,  $A_s^u = K_s/\Delta z$ ,  $A_c^u = A_n^u + A_s^u + \Delta z C_{db} a h_c |\bar{u}_J^{m-1}|$ , and the superscript  $m$  designates the  $m$ th iterative guess for the  $\bar{u}$  field. Similar results obtain for the TKE equation, and solving these equations implies the inversion of tridiagonal matrices.

Grids for mean velocity and TKE were staggered, with the lowest  $\bar{u}$  grid point falling on ground and the uppermost TKE grid point lying at  $z = 10h_c$ . Upper boundary conditions were a prescribed value ( $-1$ ) for the (normalized) momentum influx  $\overline{u'w'}/u_*^2$  and (except in the case of a wind-tunnel simulation, for which we set  $\partial k/\partial z = 0$ ) a prescribed (equilibrium) value for the normalized TKE, namely,  $k/u_*^2 = 1/c_e = 4.64$ . At the bottom boundary,  $z = 0$ , the mean wind speed  $\bar{u} = 0$ , and we imposed  $\partial k/\partial z = 0$  (flux of TKE to ground vanishes).

### d. Revisiting and confirming the Wilson et al. (1998) simulations

We carried out new simulations of the same three uniform canopy flows studied by WFR98 in developing the closure (details of these experiments can be obtained from WFR98 and references therein). Briefly, “Furry Hill” was a canopy of flexible strands of fishing line ( $h_c = 4.7$  cm), stretching upwind and over a model hill in a wind tunnel; measurements cited here are from the region upwind from the hill. The “Tombstone Canopy” was a regular array of vertical bars in the same wind tunnel, each tombstone being  $h_c = 6$  cm high by 1 cm in cross-stream width, with 6-cm cross-stream and 4.4-cm alongstream spacing. The Elora field experiment took place in a mature, uniform corn canopy of height  $h_c = 2.2$  m at Elora, Ontario, Canada.

We found that grid independence and convergence were assured in these one-dimensional canopy flow simulations, when 100 (or more) iterations were performed with grid spacing  $\Delta z = h_c/100$ . Our new simulations compared very closely to those reported by WFR98; the

differences, which were minor, we attribute to our having used higher resolution so as to attain grid independence.

### 3. Provision of the drag coefficient

The drag coefficient parameterizes the drag on the surfaces of leaves and limbs and exerts a controlling influence on the wind and turbulence among the plants. Depending on the quantity and quality of information given (the profiles of leaf area and of the flow variables  $\bar{u}$  and  $\overline{u'w'}$ ), the drag coefficient may be determined at three levels of detail.

#### a. Height-variable drag coefficient

In principle, the best way to calculate the drag coefficient, from good-quality micrometeorological measurements, would be to calculate  $C_d(z)$  by rearranging Eq. (1):

$$C_d(z) = \frac{-\frac{\partial \overline{u'w'}}{\partial z} - \frac{\partial \bar{p}}{\partial x}}{a(z)\bar{u}^2(z)}. \quad (8)$$

If we neglect the pressure gradient (which is acceptable for atmospheric flows) and normalize, we can transform the above to

$$C_d(z) = \frac{-\frac{\partial}{\partial z/h_c} \left( \frac{\overline{u'w'}}{u_*^2} \right)}{h_c a(z) \left[ \frac{\bar{u}(z)}{u_*} \right]^2} = \frac{-\Delta \left( \frac{\overline{u'w'}}{u_*^2} \right)}{\Delta \left( \frac{z}{h_c} \right) h_c a(z) \left[ \frac{\bar{u}(z)}{u_*} \right]^2}, \quad (9)$$

where the  $\Delta$  operator implies a “finite difference” along the height axis.

In the Duke Forest of KC99, mean wind and shear stress were measured at six points in and above the canopy. We calculated  $C_d$  according to Eq. (9) from the measured data  $\bar{u}/u_*$ ,  $\overline{u'w'}/u_*^2$ , and  $a(z)$  at the five sensor levels falling within the canopy. An irregular profile of  $C_d$  resulted (Fig. 1), because the observations of  $\overline{u'w'}/u_*^2$  carry considerable uncertainty and are (here, as often) given at an irregularly spaced set of points.

To alleviate this difficulty in the application of Eq. (9), one might consider “smoothly fitting” continuous polynomial curves to the measured profiles of mean wind and shear stress. Substitution of the resulting functions into Eq. (9) will then define a polynomial approximation  $C_{dp}(z)$  for the drag coefficient. In the current case, when this was tried, the outcome (Fig. 1) was unsatisfactory, giving rise to a negative drag coefficient  $C_{dp}$  deep in the canopy. Evidently this procedure requires arbitrary steps, such as the choice of order of the polynomial, in fitting what may be highly irregular profiles (e.g., the leaf area density profile reported for the Duke Forest).

Because of the irregularity of our calculated profiles of drag coefficients  $C_d(z)$  and  $C_{dp}(z)$ , we discarded Eq. (9) in favor of the following methods.

#### b. Height-averaged drag coefficient

If we have untrustworthy (or nonexistent) information on  $\overline{u'w'}$  but confidence in the profiles  $a(z)$  and  $\bar{u}(z)$ , then we can introduce a *height-averaged* drag coefficient  $\bar{C}_d$ , defined by

$$\begin{aligned} \int_0^{h_c} \frac{\partial \overline{u'w'}}{\partial z} dz &= -\tau_{h_c} + \tau(0) = -\tau_{h_c} + 0 \\ &= -\bar{C}_d \int_0^{h_c} a(z)\bar{u}(z)^2 dz, \end{aligned} \quad (10)$$

where the kinematic stress  $\tau_{h_c} = -(\overline{u'w'})_{h_c}$ . Rearrangement gives

$$\begin{aligned} \bar{C}_d &= \frac{\tau_{h_c}}{\int_0^{h_c} a(z)\bar{u}(z)^2 dz} = \frac{\tau_{h_c}/u_*^2}{\int_0^{h_c} a(z) \left[ \frac{\bar{u}(z)}{u_*} \right]^2 dz} \\ &= \frac{1}{\int_0^{h_c} a(z) \left[ \frac{\bar{u}(z)}{u_*} \right]^2 dz}. \end{aligned} \quad (11)$$

This approach avoids the differentiation of noisy  $\overline{u'w'}$  data. The value we calculate for the Duke Forest ( $\bar{C}_d = 0.2$ ; see Fig. 1) is identical to the drag coefficient cited by KC99, which may therefore be of the same provenance.

#### c. Bulk drag coefficient

If, furthermore, we have poor or nonexistent information on the leaf area density profile  $a(z)$ , then we have no choice but to use a *bulk* coefficient  $C_{da}$ , which is defined by

$$\int_0^{h_c} \frac{\partial \overline{u'w'}}{\partial z} dz = -\tau_{h_c} + 0 = -\bar{C}_d a \int_0^{h_c} \bar{u}(z)^2 dz. \quad (12)$$

By rearranging, we may define a *dimensionless* bulk coefficient  $C_{db} = h_c C_{da}$ ; that is,

$$C_{db} = \frac{1}{\int_0^1 \left( \frac{\bar{u}}{u_*} \right)^2 d \left( \frac{z}{h_c} \right)}. \quad (13)$$

Once known, this bulk drag coefficient may be utilized in a normalized momentum equation, namely,

$$\frac{\partial \overline{u'w'}/u_{*h_c}^2}{\partial(z/h_c)} = -C_{db} \left( \frac{\bar{u}}{u_*} \right)^2 - \frac{\partial(\bar{p}/u_{*h_c}^2)}{\partial x}. \quad (14)$$

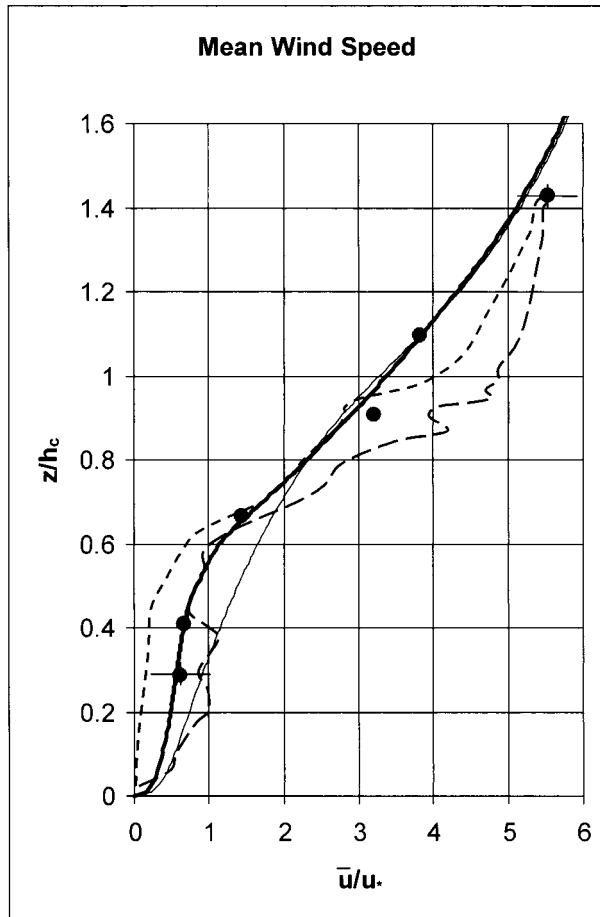


FIG. 2. Normalized mean wind speed  $\bar{u}$  of the first-order model vs observed (dots). The thick solid line is first-order closure with height-averaged  $\bar{C}_d = 0.2$ ; the thin solid line is with a bulk  $C_{db} = 0.34$ . The long-dashed line is W88; the short-dashed line is WS77 as simulated by KC99.

For the Duke Forest, Eq. (13) yields  $C_{db} = 0.34$ . We do not plot  $C_{db}$  alongside our other estimates of the drag coefficient on Fig. (1), because  $C_{db}$  has a different meaning and is imposed in a different momentum equation than are  $C_d(z)$ ,  $C_{dp}(z)$ , and  $\bar{C}_d$ .

#### 4. Comparing the first-order closure model with Duke Forest observations and the second-order simulations of Katul and Chang (1999)

Because our objective was to assess the WFR98 first-order model against the second-order models examined by KC99, in modeling the Duke Forest we followed KC99 as closely as possible (see Table 1): the top of the model domain was chosen as  $10h_c$ ; the height-averaged drag coefficient was  $\bar{C}_d = 0.2$  (same as KC99), or, where we used a bulk drag coefficient, its value was  $C_{db} = 0.34$ ; the zero-plane displacement  $d/h_c = 0.67$ ; and the normalized standard deviations  $\sigma_u/u_*$ ,  $\sigma_v/u_*$ , and  $\sigma_w/u_*$  were set respectively as 2.08, 1.86, and 1.22

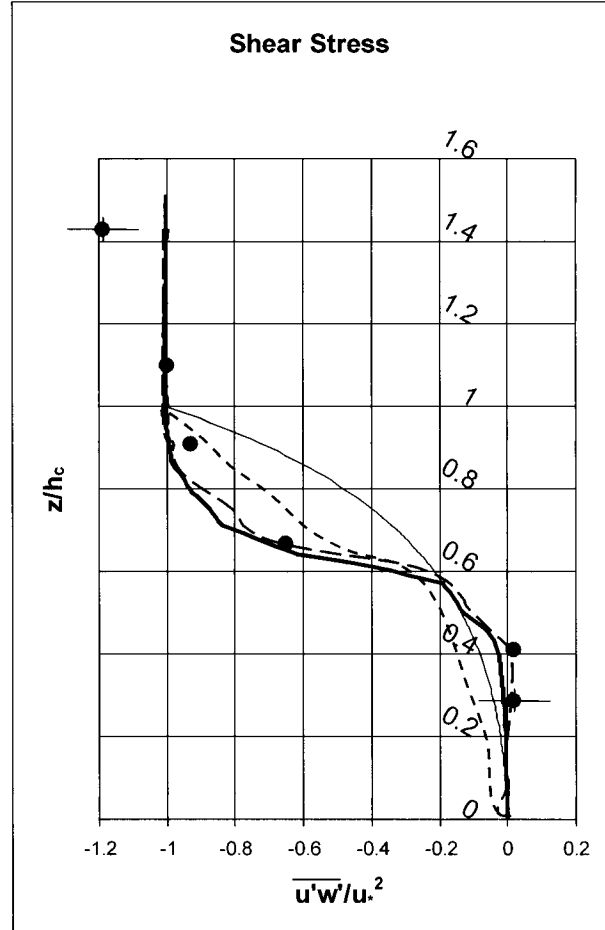


FIG. 3. The shear stress  $\overline{u'w'}$ , from the first-order model vs observed (dots). The thick solid line is first-order closure with height-averaged  $\bar{C}_d = 0.2$ ; the thin solid line is with a bulk  $C_{db} = 0.34$ . The long-dashed line is W88; the short-dashed line is WS77 as simulated by KC99.

(these being the values at  $z/h_c = 1.097$  cited in Table 3 of KC99), implying  $c_e = 1/4.64$ .

Figures 2–5 show results of our simulations of the Duke Forest; the two second-order simulations of KC99, namely WS77 and W88, have been overlaid onto the current (first-order) results for easy comparison.

Our normalized mean wind speed profile, Fig. 2, closely matches the observed profile of KC99. This result is not very surprising, given that we derived the drag coefficients (both height averaged and bulk) by integration of the observed mean wind speed profile. It should be expected, then, that the models should reproduce the mean wind and shear stress observations well. If, on the basis of Fig. 2 we are to say that the models are “good,” then perhaps the second-order models are not as good as the first-order model. The “noisiness” of the second-order solutions probably results from the absence of explicit diffusion in the momentum Eq. (1).

The first-order model also closely matches the mea-

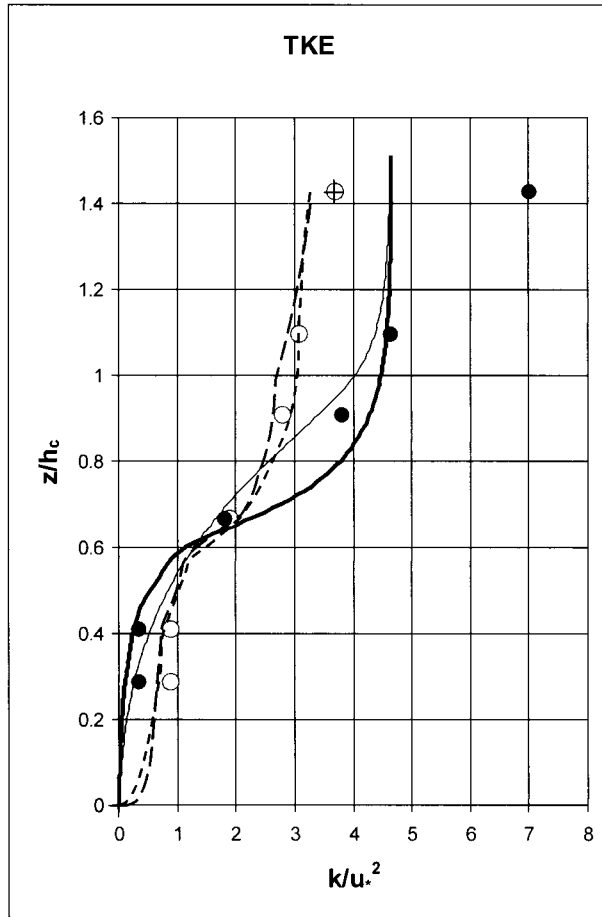


FIG. 4. The turbulent kinetic energy  $k$  of the first-order model vs observed. The solid-dot symbols are the TKE recalculated from  $\sigma_u$ ,  $\sigma_v$ , and  $\sigma_w$  given by KC99. The hollow-dot symbols are TKE given by KC99. The thick solid line is first-order closure with height-averaged  $C_d = 0.2$ ; the thin solid line is with a bulk  $C_{d,b} = 0.34$ . The long-dashed line is W88; the short-dashed line is WS77 as simulated by KC99. Note that our specification  $c_e = (k/u_*^2)_{hc}^{-1} = 1/4.64$  requires our modeled  $k$  profile to run through the observation at  $z/h_c \approx 1$ .

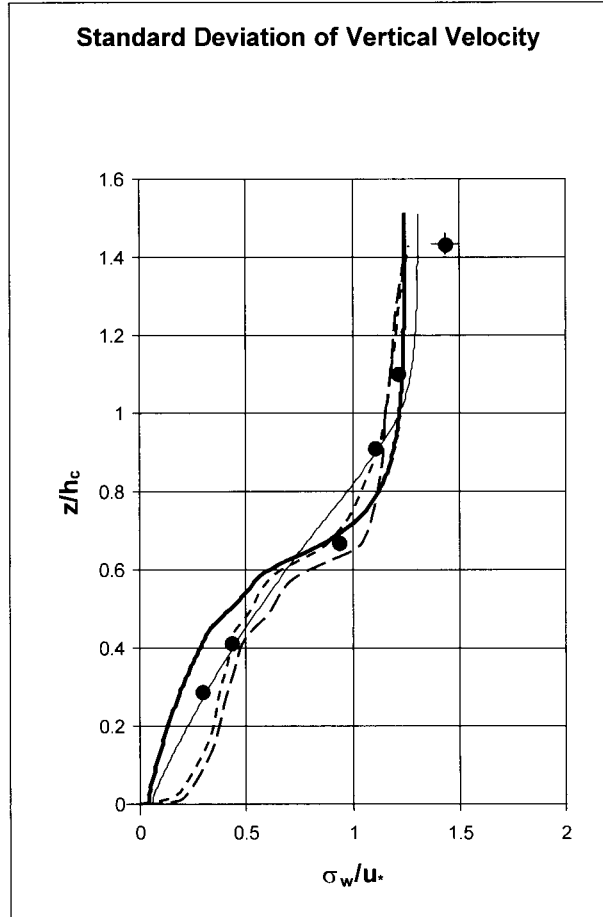


FIG. 5. Observed (dots) and modeled profiles of the normalized standard deviation of vertical velocity  $\sigma_w/u_*$ . The thick solid line is first-order closure with height-averaged drag coefficient  $\bar{C}_d = 0.2$ ; the thin solid line is with a bulk drag coefficient  $C_{d,b} = 0.34$ . The long-dashed line is W88; the short-dashed line is WS77 as simulated by KC99.

sured stress profile of KC99 (see Fig. 3) and is similar to that obtained by KC99 using the W88 model. Of course, one cannot simultaneously do a good job of the mean wind and a bad job of the shear stress, for it is implied by the way in which the drag coefficient is derived that the modeled mean wind and shear stress *must* be consistent.

Figure 4 indicates that the first-order model simulates the profile of TKE reasonably satisfactorily but underestimates the magnitude of the above-canopy TKE gradient suggested by the observations. [Note that there is a discrepancy between values of the (measured) velocity variances for Duke Forest tabulated by KC99 and the TKE they have plotted on their Fig. 1. We plot both the original and the corrected TKE on our Fig. 4.]

Except for the influence of the TKE transport term, first- and second-order models both would generate a height-invariant TKE above the canopy; for example,

just as does our Eq. (3), the TKE equation of WS77 reduces, above the canopy and provided the transport term is dropped, to  $k^{3/2} \propto u_*^2 \lambda_3 \partial \bar{u} / \partial z = \text{constant}$ . This is because  $\partial \bar{u} / \partial z \propto u_* / (z - d)$  and  $\lambda_3 \propto (z - d)$ . Thus, the differing above-canopy TKE profiles reflect the fact that treatment of TKE transport has differed, and it *may* be that our specification  $\mu = 0.2$  (recommended by WFR98, though recognizing that  $\mu = 1$  is the more frequent suggestion) has resulted in underestimation of TKE transport.

Figure 5 compares the observed vertical profile of  $\sigma_w$  in Duke Forest with simulations. Because the first-order model underestimates TKE deep in the canopy, it also underestimates the velocity variances, and thus  $\sigma_w$ .

### 5. Conclusions

The preceding results (and those of WFR98) suggest that the simpler first-order closure model will often sim-

ulate the fundamental wind properties (mean wind speed, mean shear stress, and turbulent kinetic energy) of a canopy flow as well as a second-order closure model will. The implication is that the theoretical superiority of a second-order model is moot, in the face of the large uncertainty with respect to the canopy drag coefficient that will ordinarily prevail, in any routine application of these kinds of models. Thus, bearing in mind that for two- and three-dimensional flows a second-order model is laborious, one ought not to overlook the competence of the simpler first-order model.

*Acknowledgments.* Support from the Natural Sciences and Engineering Research Council of Canada is acknowledged.

#### REFERENCES

- Katul, G. G., and W.-H. Chang, 1999: Principal length scales in second-order closure models for canopy turbulence. *J. Appl. Meteor.*, **38**, 1631–1643.
- Massman, W. J., and J. C. Weil, 1999: An analytical one-dimensional second-order closure model of turbulence statistics and the Lagrangian time scale within and above plant canopies of arbitrary structure. *Bound.-Layer Meteor.*, **91**, 81–107.
- Patankar, S. V., 1980: *Numerical Heat Transfer and Fluid Flow*. Hemisphere, 197 pp.
- Raupach, M. R., and R. H. Shaw, 1982: Averaging procedures for flow within vegetation canopies. *Bound.-Layer Meteor.*, **22**, 79–90.
- , J. J. Finnigan, and Y. Brunet, 1996: Coherent eddies and turbulence in vegetation canopies: The mixing-layer analogy. *Bound.-Layer Meteor.*, **78**, 351–382.
- Wilson, J. D., 1988: A second-order closure model for flow through vegetation. *Bound.-Layer Meteor.*, **42**, 371–392.
- , and T. K. Flesch, 1999: Wind and remnant tree sway in forest cutblocks. Part III: A windflow model to diagnose spatial variation. *Agric. For. Meteor.*, **93**, 259–282.
- , J. J. Finnigan, and M. R. Raupach, 1998: A first-order closure for disturbed plant canopy flows, and its application to windflow through a canopy on a ridge. *Quart. J. Roy. Meteor. Soc.*, **124**, 705–732.
- Wilson, N. R., and R. H. Shaw, 1977: A higher order closure model for canopy flow. *J. Appl. Meteor.*, **16**, 1197–1205.